

Effect of annealing on the properties of zinc oxide nanofiber thin films grown by spray pyrolysis technique

N. Sadananda Kumar · Kasturi V. Bangera ·
G. K. Shivakumar

Received: 19 November 2012 / Accepted: 26 December 2012 / Published online: 11 January 2013
© The Author(s) 2013. This article is published with open access at Springerlink.com

Abstract Zinc oxide nanofiber thin films have been deposited on glass substrate by spray pyrolysis technique. The X-ray diffraction studies revealed that the films are polycrystalline with the hexagonal structure and a preferred orientation along (002) direction for films annealed for 1 h at 450 °C. Further increase in annealing time changes the preferred orientation to (100) direction. The scanning electron microscopic analysis showed the formation of ZnO nanofiber with an average diameter of approximately 800 nm for annealed films. The compositional analysis of nanofiber ZnO thin films were studied by time of flight secondary ion mass spectroscopy, which indicated oxygen deficiency in the films. The optical properties of annealed films have shown a variation in the band gap between 3.29 and 3.20 eV. The electrical conductivity of the as grown and annealed films showed an increase in the conductivity by two orders of magnitude with increase in annealing duration.

Keywords Zinc oxide · Spray pyrolysis · Nanofibers · Annealing time · Optical properties

Abbreviations

ZnO	Zinc oxide
XRD	X-ray diffractometer
SEM	Scanning electron microscope
AFM	Atomic force microscope
TOFSIMS	Time of flight secondary ion mass spectroscopy

TCO	Transparent conducting oxide
FWHM	Full width at half maximum
RMS	Root mean square
T_g	Glass transition temperature
E_u	Urbach energy
meV	Milli electron volt
$I-V$	Current–voltage
E_g	Energy band gap
σ	Conductivity
% T	% Transmittance

Introduction

Zinc oxide (ZnO) is one of the most important semiconductor materials belonging to II–VI group. It is a direct wide band gap semiconductor (3.37 eV) and it has high exciton binding energy of 60 meV (Look 2001). Due to the wide range of optical and electrical properties, ZnO thin films are of technological importance (Ayouchi et al. 2003). ZnO thin films have many advantages: high chemical and mechanical stability, nontoxic in nature, high abundance, and transparency over other oxide thin films like ITO, CdO, SnO₂, etc. ZnO is used as transparent conductive oxide (TCO) thin films, mainly in solar cells (Ohta et al. 2011), heat mirrors, and organic light emitting diodes (Gong et al. 2010; Yoo et al. 2008). It can also be used as piezo electric devices and gas sensors (Kang and Joung 2007; Ferro 2009). Different methods have been employed to prepare the ZnO thin films, such as sputtering (Mahmood et al. 1995; Liu et al. 2007), thermal evaporation (Ma et al. 1996), sol–gel method (Tsay et al. 2010), electron beam evaporation method (Varnamkhasti et al. 2012), pulsed laser evaporation (Zhao et al. 2006), and

N. Sadananda Kumar (✉) · K. V. Bangera · G. K. Shivakumar
Thin films Laboratory, Department of Physics, National Institute of technology Karnataka, Surathkal, 575025 Mangalore, India
e-mail: sadanthara@gmail.com

spray pyrolysis technique (Lokhande et al. 2002; Alver et al. 2007; Sahay and Nath 2008).

The spray pyrolysis is simple and inexpensive technique to prepare the ZnO thin films and it is useful for large area applications. In the present study, we report the deposition of ZnO nanofibers on glass substrate and the effect of annealing time on structural, morphological, optical, and electrical properties of the ZnO nanofibers.

Experimental details

ZnO nanofiber films were prepared on cleaned glass substrate using spray pyrolysis technique. The starting solution was prepared using 0.05 M zinc acetate anhydrous $\text{Zn}(\text{CH}_3\text{COO})_2$ in methanol and water in the ratio of 3:1. The small quantity of acetic acid is added to avoid the formation of $\text{Zn}(\text{OH})_2$ precipitate. This solution was sprayed on to the heated glass substrate by means of spray nozzle at the constant pressure of 0.2 Torr. The deposition of ZnO thin films has been carried out at a constant temperature of 450 ± 5 °C, with air as the carrier gas. The separation between the substrate and nozzle was optimized to get the uniform film deposition.

Thickness of the deposited film was determined using gravimetric method. Film thickness of around 1 μm is used in the present study. The structural characterization of the film was carried out using X-ray diffractometer with $\text{Cu } k_\alpha$ radiation of wavelength $\lambda = 1.5418$ Å. The influence of annealing time on the structure of ZnO nanofiber thin films was investigated. The crystallite size was calculated from the Scherrer's formula. Scanning electron microscope

(SEM) and atomic force microscope (AFM) have been used to study the surface morphology and topography of the nanofiber thin films. The compositional analysis of as grown and annealed films has been studied using time of flight secondary ion mass spectroscopy (TOFSIMS). The transmittance spectra of the as grown and annealed films were studied using UV–visible spectrophotometer. The electrical properties of the films were determined using Keithley multimeter and source meter.

Results and discussions

Structural characterizations

Figure 1 shows the XRD patterns of as grown film and films annealed for various time durations. It was observed that all the films exhibit hexagonal wurtzite polycrystalline structure. The as-grown film has got the preferred orientation along the (002) direction. Films annealed for 1 h showed an increase in the intensity along (002) direction but when annealed for 4 h it changes to (100) direction with increase in intensity of the peak. The average crystallite size of the wurtzite phase was estimated from the high intensity peak in the XRD patterns using Scherrer's formula (Maity et al. 2005):

$$D = \frac{0.9\lambda}{\beta \cos \theta} \quad (1)$$

where ' λ ' is the wavelength of X-rays, ' θ ' is the Bragg's angle in radians, and ' β ' is the full width at half maximum (FWHM) of the high intensity peak. The lattice constants

Fig. 1 XRD pattern of as grown and annealed films

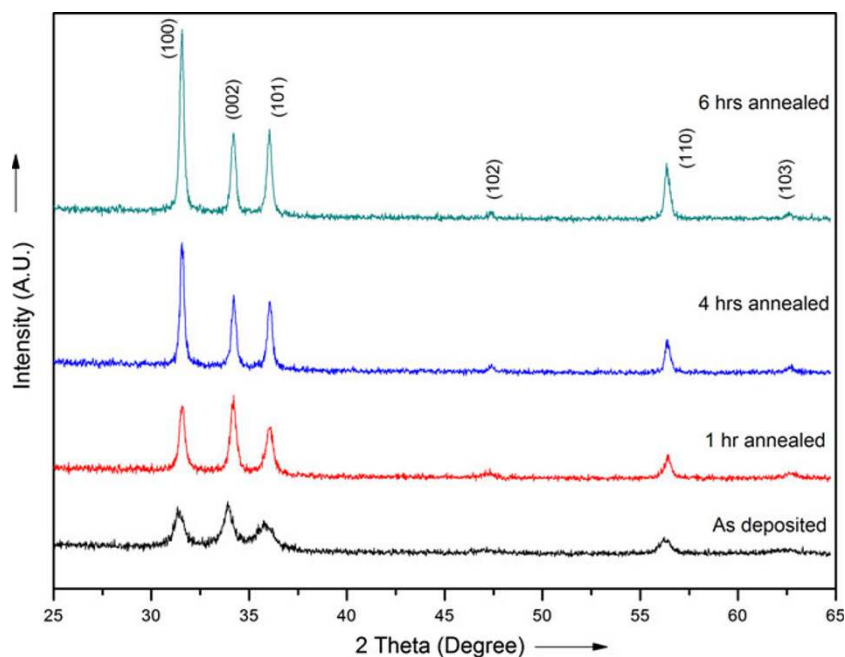
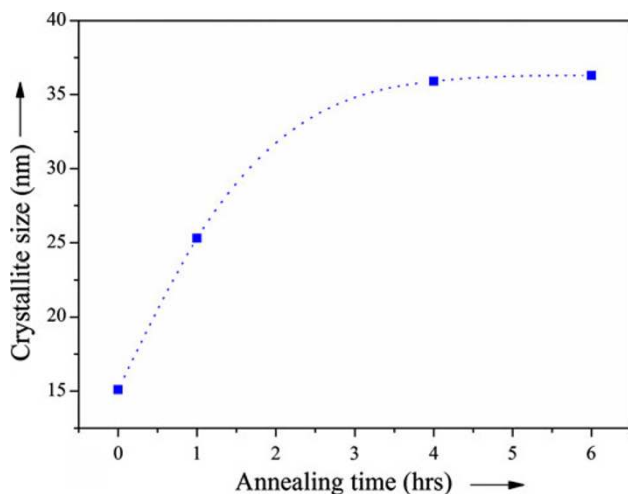


Table 1 XRD data of as grown and annealed ZnO thin films

Annealing time (h)	%T	σ (S m ⁻¹)	E_g (eV)	E_u (meV)
0	75	0.6	3.29	377
1	79	16.0	3.28	264
4	72	79.9	3.24	210
6	66	91.2	3.20	278

**Fig. 2** Variation of crystallite size with annealing time

a and c can be calculated for the high intensity peaks using the formula (Ilican et al. 2006).

$$\frac{1}{d^2} = \frac{4(h^2 + k^2 + hk)}{3a^2} + \frac{l^2}{c^2} \quad (2)$$

The calculated values are listed in Table 1, and are in agreement with the JCPDS file: zinc oxide, 80-0074 ($a = 3.2535 \text{ \AA}$ and $c = 5.2151 \text{ \AA}$).

The calculated values of crystallite size are also given in Table 1. It is noted that average grain size of as-deposited film is 15.1 nm, which increases from 25.3 to 36.3 nm as the annealing time duration increases from 1 to 6 h, respectively. This indicates an improvement in the crystalline nature of the film with increase in annealing time duration. According to Cavalcante et al. (2007), the growth of granules with the increase of annealing time promotes the reduction of the number of non-bridging oxygen type defects favouring the formation of the ZnO grains. Figure 2 depicts the variation of crystallite size with annealing time.

The dislocation density can be defined as length of the dislocation lines per unit volume of crystal, which is calculated from the Williamson and Smallman's (1956) relation:

$$\delta = \frac{1}{D^2} \quad (3)$$

where D is the crystallite size. It was observed that dislocation density δ decreases with the increase in annealing

time as shown in Table 1, which indicates reduction in defects with increasing annealing duration. The small values of δ or high values of D indicate the good crystallinity of the nanofiber ZnO thin films.

Morphological study

Figure 3 shows the SEM images of as-grown and annealed ZnO nanofiber films. The average diameter of the nanofiber in the as-grown film was found to be approximately 300 nm, whereas the average diameter of fiber in the 6 h annealed film was approximately 800 nm. Maity et al. (2005) obtained the nanofiber thin films, with an average diameter of 500 nm. Ilican et al. (2006) also reported the indium-doped zinc oxide nanofibers with uniform diameter of 200 nm. But in the present study, the average diameter of the nanofiber in the as-grown film and in the annealed film was found to be 300 and 800 nm, respectively. It was found that the average diameter of the fibers increases with annealing time, which is probably due to agglomeration of finer fiber during annealing process, producing thicker fibers. It has been observed that the annealing temperature has a direct influence on the thickness of the fibres (Maity et al. 2005).

The improvement in the structural order of ZnO thin films with increase in the annealing time was also confirmed by AFM analysis. The improvement in the structural order may be due to the reduction of non-bridging oxygen type defects, which favours the formation of hexagonal structure (Cavalcante et al. 2007). The surface roughness of as deposited and annealed films was also determined. Figure 4 shows the variation of RMS surface roughness with annealing time. It was found that RMS surface roughness increases with increasing annealing time. This may be due to evaporation of water during thermal annealing (Regragui et al. 2001). This is in agreement with the SEM study which shows increase in the size of fibers with increasing annealing duration.

Compositional analysis

The compositional analysis of ZnO nanofiber thin films have been studied using TOFSIMS. Depth profile spectra of as-grown and annealed ZnO thin films have been analysed in a raster $400 \times 400 \mu\text{m}^2$ area. The depth profile studies were made of as deposited and films annealed at $450 \text{ }^\circ\text{C}$ for 6 h. It was observed that percentage of Zn is increased after annealing. This suggests that percentage of oxygen in the annealed films decreases due to annealing. Thus, annealed films were oxygen deficient.

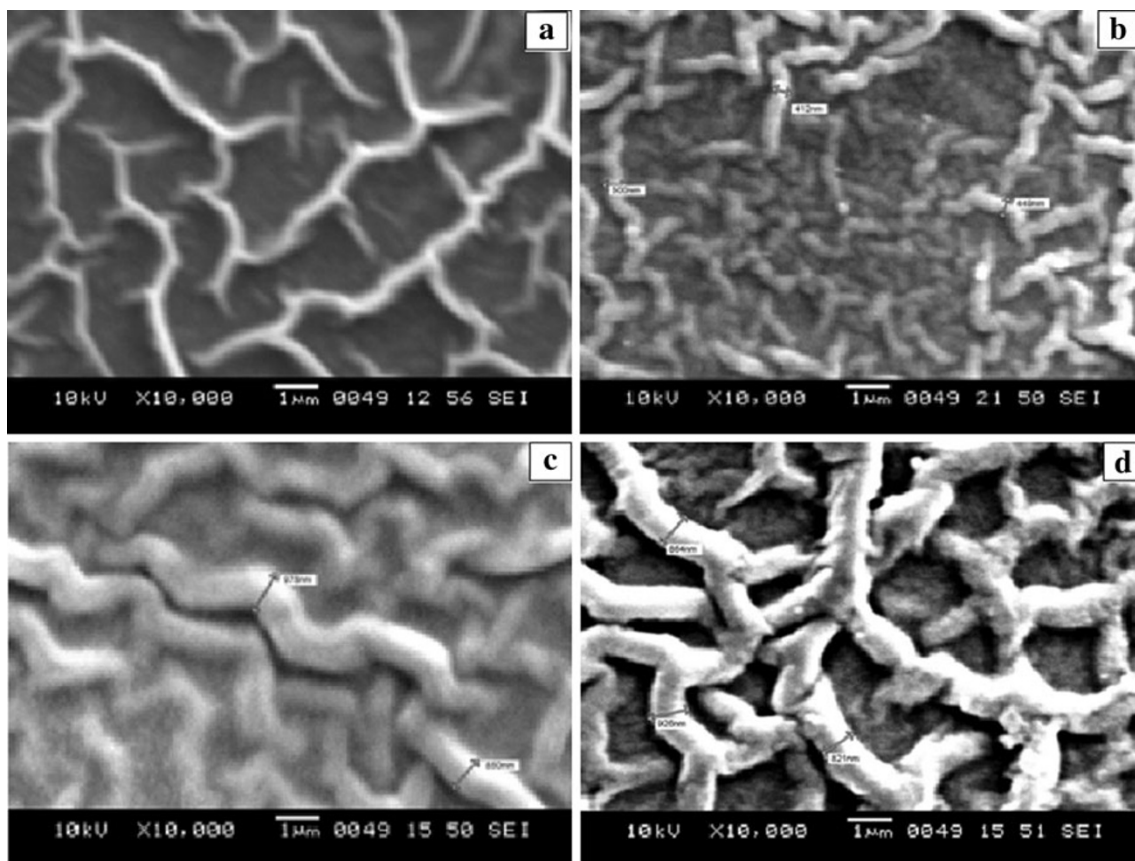


Fig. 3 SEM images of **a** as grown ZnO thin film, **b** 1 h annealed, **c** 4 h annealed film, **d** 6 h annealed film

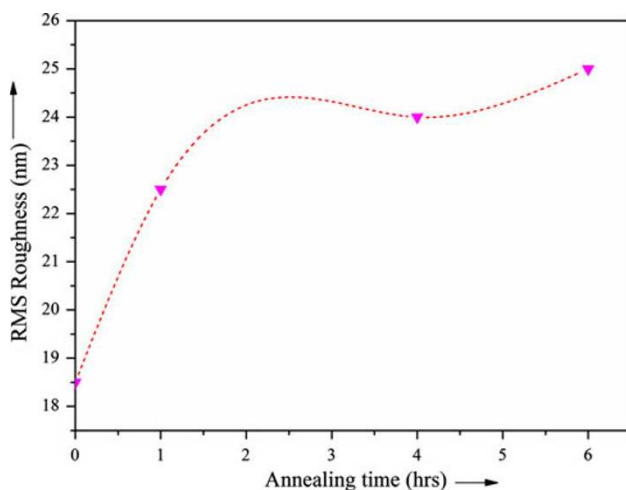


Fig. 4 Variation of RMS surface roughness with annealing time

Optical characterization

Optical transmittance spectra of ZnO nanofiber thin films annealed for different time durations were shown in the Fig. 5. It is observed that the obtained films have uniform thickness indicated by absence of the interference pattern in the transmittance graph. The as-grown films show the

75 % transmittance in the visible region. The transmittance of the films annealed for 1 h has showed an increase in the transmittance up to 79 %. Further increase in the annealing time up to 6 h reduces the transmittance to 66 %. This is associated with increased evaporation of water, the effect on surface roughness and defects as reported by Rezagui et al. (2001). Absorption coefficient (α) was determined at the region of strong absorption from the transmittance data, as follows (Joseph et al. 1999).

$$\alpha = \ln \left(\frac{1}{T} \right) / t \quad (4)$$

where T is the transmittance of the film and t is the thickness of the film. The optical band gap of the annealed films for different time duration was calculated using the transmission spectra. The relation between the optical band gap (E_g) and absorption coefficient (α) is given by (Joseph et al. 1999).

$$\alpha h\nu = B(h\nu - E_g)^n \quad (5)$$

where $h\nu$ is the photon energy, B is proportionality constant and the exponent n depends on the type of optical transition which is $1/2$ for all allowed direct transition. The variation of $(\alpha h\nu)^2$ with $h\nu$ for the as-grown and annealed films has

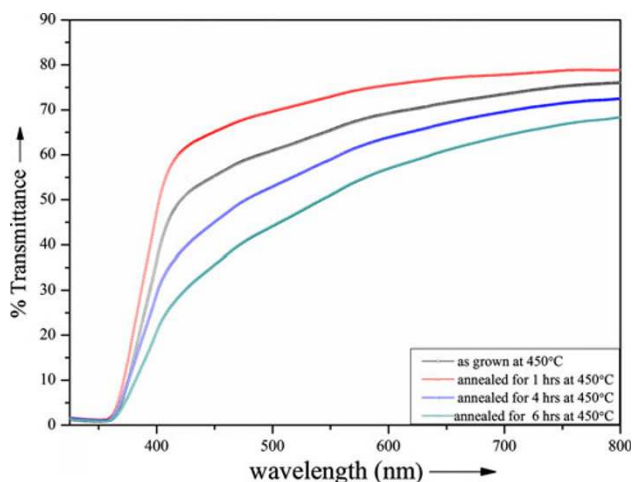
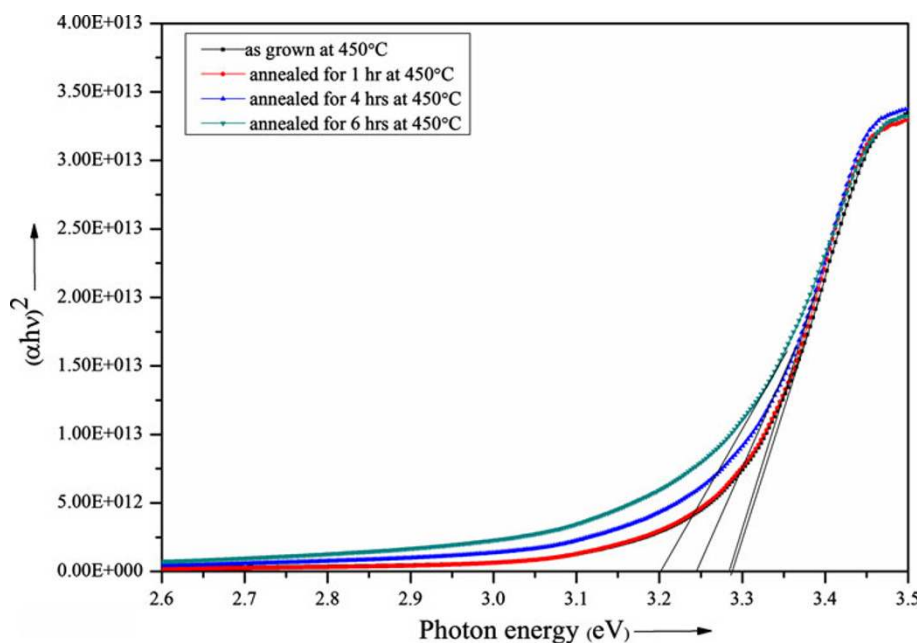


Fig. 5 Transmittance spectra of as grown and annealed ZnO thin films

been shown in the Fig. 6 and is found to be linear which indicates that the transition is direct. The extrapolation of linear part of $(\alpha hv)^2$ with hv plot to $\alpha = 0$, gives the optical band gap of the nanofiber thin films.

The band gap of as-grown film was found to be 3.29 eV, which decreases to 3.20 eV, as the annealing time increases up to 6 h as shown in Table 2. According to reports, decrease in the band gap occurs due to the appearance of band tail resulting from defects associated with the presence of cavities and surface roughness (Regragui et al. 2001). The decrease in the band gap with annealing time was also observed in chalcogenide films (Hafiz et al. 1998; Abu-Sehly 2000). It was known that during thermal annealing at temperatures below the glass transition

Fig. 6 Variation of $(\alpha hv)^2$ with hv of as grown and annealed ZnO thin films



temperature T_g , the unsaturated defects are gradually annealed producing a larger number of saturated bonds. The reduction in the number of unsaturated defects decreases the density of localized states in the band structure (Siciliano et al. 2010).

The optical transition between the occupied state in the valance band tail and unoccupied state in the conduction band edge is explained by the following equation (Caglar et al. 2007).

$$\alpha = \alpha_o \exp(hv/E_u) \tag{6}$$

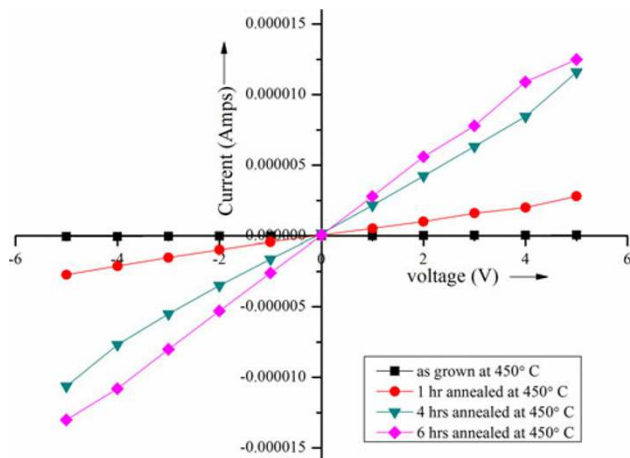
where α_o is a constant and E_u is the Urbach energy which characterizes the slope of the exponential edge. The inverse of the slope of $\ln \alpha$ with i plot gives the value of Urbach energy (E_u) and the calculated values are given in Table 2. The Urbach energy of as-deposited film is 376.5 meV. It was found that the E_u decreases slightly with increasing annealing time up to 4 h; this suggests that the crystallinity of nanofiber thin films improved by reducing the defects present in the film.

Electrical characterization

The electrical characterizations of as-deposited and annealed films were carried out using two probe methods using silver as a contact electrode. The variation of current with voltage was noted between -5 and 5 V. The variation of current with voltage of as-grown and annealed films for different time duration has been shown in the Fig. 7. It was found that both the as-grown and the annealed films have linear $I-V$ curve, indicating that conduction mechanism is ohmic. The transmittance, electrical conductivity, and

Table 2 The variation of transmittance, conductivity, Urbach energy and band gap of as grown and annealed ZnO nanofiber thin films

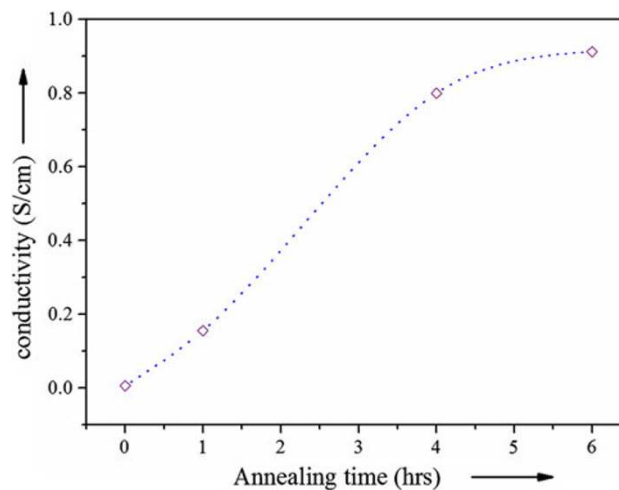
Material	% Transmittance	Conductivity (S/m)	References
ZnO	74	79.9	
AZO	80	35.7×10^3	Muiva et al. (2011)
ITO	80	34.3×10^3	Manoj et al. (2007)

**Fig. 7** I-V graph of as grown and annealed films

energy band gap of as-grown and annealed films were presented in Table 2. It was observed that the as-grown films have low conductivity, which may be due to grain boundary effects and also, due to adsorption of air was used as carrier gas. There is a possibility of chemisorptions of large number of oxygen molecules on the surface and grain boundaries of the film, which will create the potential barrier that affects the electrical transport causing a reduction in conductivity (Joseph et al. 1999).

To improve the conductivity of the as-grown ZnO thin films, they were annealed at 450 °C for different time durations. On annealing, there may be desorption of chemisorbed oxygen ions from the samples, donating an electron to the atom causing increase in the conductivity by reducing the grain boundary potential. The electrical conductivity depends on the number of charge carriers and mobility (Bouhssira et al. 2006). Due to the increase in crystallite size, grain boundary density decreases and mobility of the thin films increases. The variation of conductivity with the annealing time was shown in the Fig. 8. The conductivity of the as-grown ZnO thin film was 0.6 S m^{-1} , and it increased to a value 91.2 S m^{-1} when the films were annealed for 6 h at 450 °C.

In order to attain the transparency of the films about 90 % in the visible region, film thickness should be reduced to 425 nm. Conductivity of these films is found to be

**Fig. 8** Variation of conductivity with the annealing time**Table 3** Comparison of transmittance and conductivity data of present work with other reports

Growth method	% Transmittance	Conductivity (S/m)	References
Present work	74	79.9	
Spray pyrolysis	75	15×10^{-3}	Ilican et al. (2006)
Sol gel	80	2.4×10^{-9}	Mansour and Yakuphanoglu (2012)
Catalyst free solution route	70	–	Maity et al. (2005)

23.2 S m^{-1} . The decrease in the conductivity is due to difference in the film thickness (Prasada Rao and Santhoshkumar 2009). Growth of undoped and doped ZnO nanofibers using different techniques has been reported (Maity et al. 2005; Ilican et al. 2006; Mansour and Yakuphanoglu 2012). The conductivity and transmittance data of their work are compared with the present work and shown in Table 3. It is noted that nanofiber films grown in the in present work have high conductivity with comparable transmittance to that of other groups. The comparison of conductivity of ZnO films with that of AZO (Muiva et al. 2011) and ITO (Manoj et al. 2007) films is shown in Table 4. Since the deposited films are undoped, conductivity of the films are less than that of AZO and ITO films. Doping of III group elements like Al, In or Ga to ZnO is expected to improve the conductivity without affecting transmittance of the films.

Conclusions

ZnO nanofiber thin films were deposited on the glass substrate successfully by spray pyrolysis technique. XRD

Table 4 Comparison of transmittance and conductivity data of ZnO with AZO and ITO

Annealing time (h)	Angle (°2θ)	Orientation	D (nm)	$\delta \times 10^{-5}$ (1/Å ²)	a (Å)	c (Å)
0	31.30	(002)	15.1	4.39	3.30	5.28
1	31.62	(002)	25.3	1.56	3.27	5.24
4	31.57	(100)	35.9	0.78	3.27	5.24
6	31.55	(100)	36.7	0.74	3.27	5.24

pattern of annealed ZnO nanofiber thin films exhibits good crystalline structure with (100) preferred orientation. SEM image showed the formation of ZnO nanofibers with the average diameter of 300–800 nm. TOFSIMS analysis reveals the oxygen deficiency of annealed nanofiber thin films. AFM analysis shows that the RMS roughness of nanofibers increased with increasing annealing time. The optical properties of the nanofiber thin films showed a dependence of annealing time. The energy band gap of ZnO thin films decreases from 3.29 to 3.20 eV with increase in the annealing time. The conductivity of the ZnO nanofiber thin films found to be increase with increase in the annealing time. Hence, annealed ZnO nanofiber thin films may be useful as transparent conducting oxide contact for solar cells.

Acknowledgments We thank the Department of Materials Science and Metallurgical Engineering IIT Madras for providing AFM facility. We also thank the SAIF IIT Bombay for helping in TOFSIMS study.

Open Access This article is distributed under the terms of the Creative Commons Attribution License which permits any use, distribution, and reproduction in any medium, provided the original author(s) and the source are credited.

References

- Abu-Sehly AA (2000) Optical constants and electrical conductivity of Ge₂₀Se₆₀Sb₂₀ thin films. *J Mater Sci* 35:2009–2013
- Alver U, Kilinc T, Bacaksiz E, Kucukomeroglu T, Nezir S, Mutlu İH, Aslan F (2007) Synthesis and characterization of spray pyrolysis zinc oxide microrods. *Thin Solid Films* 515:3448–3451. doi:10.1016/j.tsf.2006.10.016
- Ayouchi R, Leinen D, Martín F, Gabas M, Dalchiele E, Ramos-Barrado JR (2003) Preparation and characterization of transparent ZnO thin films obtained by spray pyrolysis. *Thin Solid Films* 426:68–77. doi:10.1016/S0040-6090(02)01331-7
- Bouhssira N, Abed S, Tomasella E, Cellier J, Mosbah A, Aida MS, Jacquet M (2006) Influence of annealing temperature on the properties of ZnO thin films deposited by thermal evaporation. *Appl Surf Sci* 252:5594–5597. doi:10.1016/j.apsusc.2005.12.134
- Caglar Y, Ilican S, Caglar M, Yakuphanoglu F (2007) Effects of In, Al and Sn dopants on the structural and optical properties of ZnO thin films. *Spectrochim Acta Part A* 67:1113–1119. doi:10.1016/j.saa.2006.09.035
- Cavalcante LS, Anicete-Santos M, Pontes FM, Souza IA, Santos LPS, Rosa ILV, Santos MRMC, Santos-Júnior LS, Leite ER, Longo E (2007) Effect of annealing time on morphological characteristics of Ba(Zr,Ti)O₃ thin films. *Alloys Compd* 437:269–273. doi:10.1016/j.jallcom.2006.07.100
- Ferro R (2009) The effect of the material morphology on the response of the NO₂ sensor based on ZnO thin film. *Sens Actuators B* 143:99–102. doi:10.1016/j.snb.2009.09.025
- Gong L, Ye Z, Lu J, Zhu L, Huang J, Gu X, Zhao B (2010) Highly transparent conductive and near-infrared reflective ZnO: Al thin films. *Vacuum* 84:947–952. doi:10.1016/j.vacuum.2010.01.010
- Hafiz MM, Abdel-Rahim MA, Abu-Sehly AA (1998) Optical absorption and electrical conductivity of amorphous AsTeGe thin films. *Phys B* 252:207–215. doi:10.1016/S0921-4526(98)00053-2
- Ilican S, Caglar Y, Caglar M, Yakuphanoglu F (2006) Electrical conductivity, optical and structural properties of indium-doped ZnO nanofiber thin film deposited by spray pyrolysis method. *Physica E* 35:131–138. doi:10.1016/j.physe.2006.07.009
- Joseph B, Gopchandran KG, Manoj PK, Koshy P, Vaidyan VK (1999) Optical and electrical properties of zinc oxide films prepared by spray pyrolysis. *Bull Mater Sci* 22:921–926
- Kang SJ, Joung YH (2007) Influence of substrate temperature on the optical and piezoelectric properties of ZnO thin films deposited by rf magnetron sputtering. *Appl Surf Sci* 253:7330–7335. doi:10.1016/j.apsusc.2007.03.020
- Liu ZW, Sun CW, Zhang QY, Wang YN, Wu B, Jin ZX (2007) Morphology and interface characteristics of ZnO films deposited at room temperature and 750 °C. *Surf Coats Technol* 201:5422–5426. doi:10.1016/j.surfcoat.2006.07.049
- Lokhande BJ, Patil PS, Uplane MD (2002) Deposition of highly oriented ZnO films by spray pyrolysis and their structural. Optical and electrical characterization. *Mater Lett* 57:573–579. doi:10.1016/S0167-577X(02)00832-7
- Look DC (2001) Recent advances in ZnO materials and devices. *Mater Sci Eng B* 80:383–387. doi:10.1016/S0921-5107(00)00604-8
- Ma J, Feng Ji HM, Li SY (1996) Electrical and optical properties of ZnO: Al films prepared by an evaporation method. *Thin Solid Films* 279:213–215. doi:10.1016/0040-6090(95)08173-9
- Mahmood FS, Gould RD, Hassan AK, Salih HM (1995) D.C. properties of ZnO thin films prepared by r.f. magnetron sputtering. *Thin Solid Films* 270:376–379. doi:10.1016/0040-6090(95)06928-3
- Maity R, Das S, Mitra MK, Chattopadhyaya KK (2005) Synthesis and characterization of ZnO nano/microfibers thin films by catalyst free solution route. *Physica E* 25:605–612. doi:10.1016/j.physe.2004.09.002
- Manoj PK, Joseph B, Vaidyan VK, Sumangala Devi Amma D (2007) Preparation and characterization of indium-doped tin oxide thin films. *Ceramics Int* 33:273–278. doi:10.1016/j.ceramint.2005.09.016
- Mansour ShA, Yakuphanoglu F (2012) Electrical-optical properties of nanofiber ZnO film grown by sol gel method and fabrication of ZnO/p-Si heterojunction. *Solid State Sci* 14:121–126. doi:10.1016/j.solidstatesciences.2011.11.007
- Muiva CM, Sathiaraj TS, Maabong K (2011) Effect of doping concentration on the properties of aluminium doped zinc oxide thin films prepared by spray pyrolysis for transparent electrode applications. *Ceramics Int* 37:555–560. doi:10.1016/j.ceramint.2010.09.042
- Ohta N, Ohba D, Sato S, Tang Z, Shimizu H, Shirai H (2011) Rapid thermal-plasma annealing of ZnO: Al films for silicon thin film

- solar cells. *Thin Solid Films* 519:6920–6927. doi:[10.1016/j.tsf.2011.04.043](https://doi.org/10.1016/j.tsf.2011.04.043)
- Prasada Rao T, Santhoshkumar MC (2009) Effect of thickness on structural, optical and electrical properties of nanostructured ZnO thin films by spray pyrolysis. *Appl Surf Sci* 255:4579–4584. doi:[10.1016/j.apsusc.2008.11.079](https://doi.org/10.1016/j.apsusc.2008.11.079)
- Regragui M, Addou M, El Idrissi B, Bernède JC, Outzourhit A, Echamikh E (2001) Effect of the annealing time on the physico-chemical properties of WO₃ thin films by spray pyrolysis. *Mater Chem Phys* 70:84–89. doi:[10.1016/S0254-0584\(00\)00464-8](https://doi.org/10.1016/S0254-0584(00)00464-8)
- Sahay PP, Nath RK (2008) Al doped ZnO thin films as methanol sensors. *Sens Actuators B* 134:654–659. doi:[10.1016/j.snb.2008.06.006](https://doi.org/10.1016/j.snb.2008.06.006)
- Siciliano T, Di Giulio M, Tepore M, Filippo E, Micocci G, Tepore A (2010) Effect of thermal annealing time on optical and structural properties of TeO₂ thin films. *Vacuum* 84:935–939
- Tsay C-Y, Fan K-S, Chen S-H, Tsaif C-H (2010) Preparation and characterization of ZnO transparent semiconductor thin films by sol-gel method. *J. Alloys Compd.* 495:126–130. doi:[10.1016/j.jallcom.2010.01.100](https://doi.org/10.1016/j.jallcom.2010.01.100)
- Varnamkhasti MG, Fallah HR, Zadsar M (2012) Effect of heat treatment on characteristics of nanocrystalline ZnO films by electron beam evaporation. *Vacuum* 86:871–875. doi:[10.1016/j.vacuum.2011.03.017](https://doi.org/10.1016/j.vacuum.2011.03.017)
- Williamson GB, Smallman RC (1956) Dislocation densities in some annealed and cold-worked metals from measurements on the X-ray debye-scherrer spectrum. *Phil Mag* 1:34–46. doi:[10.1080/14786435608238074](https://doi.org/10.1080/14786435608238074)
- Yoo D-G, Nam S-H, Kim MH, Jeong SH, Jee H-G, Lee HJ, Lee N-E, Hong BY, Kim YJ, Jung D, Boo J-H (2008) Fabrication of the ZnO thin films using wet-chemical etching processes on application for organic light emitting diode (OLED) devices. *Surf Coats Technol* 202:5476–5479. doi:[10.1016/j.surfcoat.2008.06.064](https://doi.org/10.1016/j.surfcoat.2008.06.064)
- Zhao J-L, Li X-M, Bian J-M, Yu W-D, Zhang C-Y (2006) Comparison of structural and photoluminescence properties of ZnO thin films grown by pulsed laser deposition and ultrasonic spray pyrolysis. *Thin Solid Films* 515:1763–1766. doi:[10.1016/j.tsf.2006.06.032](https://doi.org/10.1016/j.tsf.2006.06.032)